Pete's Thesis

by

Peter Thompson

A thesis submitted in conformity with the requirements
for the degree of Doctor of Philosophy
Graduate Department of Physics
University of Toronto

Abstract

Pete's Thesis

Peter Thompson

Doctor of Philosophy

Graduate Department of Physics

University of Toronto

2011

(At most 150 words for M.Sc. or 350 words for Ph.D.)

Contents

Chapter 1

The Standard Model

1.1 Overview

The Standard Model (SM) describes the particles present in nature and the interactions between them. It has existed in it's current form since 1978, and has been validated by numerous experiments since

Elementary particles in the standard model are divided into two groups: the quarks and leptons. These particles represent the fundamental building blocks of matter, and there are six "flavours" of each. For the quarks these are the up (u), down (d), charm (c), strange (s), top (t), and bottom (b). These may be organised into three mass generations as follows

$$\begin{pmatrix} u \\ d \end{pmatrix} \quad \begin{pmatrix} c \\ s \end{pmatrix} \quad \begin{pmatrix} t \\ b \end{pmatrix}, \tag{1.1}$$

where the upper members of each generation have charge +2/3 and the lower members have charge -1/3. The leptons may be arranged in the same way, giving

$$\begin{pmatrix} \nu_e \\ e \end{pmatrix} \quad \begin{pmatrix} \nu_\mu \\ \mu \end{pmatrix} \quad \begin{pmatrix} \nu_\tau \\ \tau \end{pmatrix}, \tag{1.2}$$

where the lower members are the electron, muon, and tau, respectively, each having charge -1. Each of these is paired with a neutrino (ν_x), which is neutral and (almost) massless. Quarks and leptons are both fermions, with all twelve of these particles having spin 1/2.

The strong, weak, and electromagnetic forces are also described by the standard model[1]. These are described by gauge theories, such that the SM Lagrangian exhibits $SU(3)_c \otimes SU(2)_L \otimes U(1)_Y$ symmetry. The doublets listed in equations 1.1 and 1.2 reflect the way in which the quark and lepton fields transform under the $SU(2)_L$ symmetry group, where the subscript L denotes that only the left handed components of the fields take part in this interaction.

Interactions between particles may occur via the strong (or colour) force, the weak force, and the electromagnetic force. These interactions are described in terms of gauge bosons, which act as force carriers and all have spin 1. The strong force is carried by gluons, which are massless. There are eight types of gluon, corresponding to the 8 generators of the $SU(3)_c$ symmetry associated with the strong force. There would be four massless bosons arising from the $SU(2)_L o \times U(1)_Y$ symmetries, however these symmetries are broken down to a single $U(1)_{EM}$ symmetry by the Higgs mechanism. This $U(1)_{EM}$ symmetry describes electromagnetic interactions, and the corresponding gauge boson is the massless photon. The other three gauge bosons associated with the broken symmetries are the W^+/W^- bosons which have a mass of 80GeV, and the Z_0 boson which has a mass of 91 GeV.

In addition to the gauge bosons, the standard model also describes a Higgs boson. The Higgs field allows the fermionic particles (and the gauge bosons of the weak force) to posses mass in a way that doesn't violate the gauge invariance of the SM Lagrangian. It is this mechanism that is responsible for the breaking of the electroweak ($SU(2)_L \otimes U(1)_Y$) symmetry. The Higgs field has a potential that makes it favorable for it to take a non

[1] gravity is not included in the SM, but its effects are negligible at the energy scales of interest.

zero vacuum expectation value. Fermions and gauge bosons then interact with the Higgs field via a Yukawa coupling, and so when the Higgs takes a vev these couplings act as mass terms in the Lagrangian, while retaining their gauge invariance. At present the Higgs boson is the only particle in the standard model that has not been experimentally observed. However, The ATLAS experiment has narrowed the mass range of the Higgs boson to be within 115-131 GeV[4]. If the Higgs boson exists, it is expected to be observed at ATLAS by the end of 2012.

1.2 Quantum ChromoDynamics

The physics of the strong force are described by Quantum ChromoDynamics (QCD), which is a gauge theory based on the symmetry group $SU(3)_c$. It is the strongest of the three interactions in the standard model, and effects quarks but not leptons. As the LHC collides beams of protons, QCD is the dominant interaction. LHC collides protons, therefore QCD is dominant interaction. QCD: non abelian gauge theory of $SU(3)$. As mentioned above, gauge particles are gluons, of which there are 8 types.

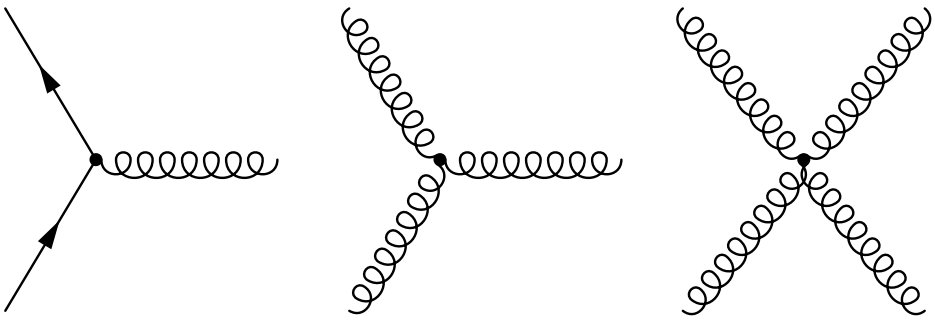

Figure 1.1: Feynman diagrams depicting the vertices of QCD.

Feynman diagrams for QCD vertices are shown in figure 1.3. A major difference of QCD compared to quantum electrodynamics (QED) is that gluons carry colour charge and thus interact with themselves, while the photon is chargeless. Gluon-gluon interac-

tions can occur via the three gluon or four gluon vertices, which are depicted in figures 1.1(b) and 1.1(c).

The coupling constant, α_s, describes the strength of QCD interactions. This varies as a function of momentum, such that the strength of the coupling at two different momentum scales, q^2 and Q^2, are related by

$$\alpha_s(q^2) = \frac{\alpha_s(Q^2)}{1 + \frac{11-2/3N_f}{4\pi}\alpha_s(Q^2)\log(\frac{q^2}{Q^2})} \tag{1.3}$$

where N_f is the number of quark flavours with mass less than q^2 and Q^2. The "QCD scale", Λ_{QCD} , is defined as the scale at which the denominator of equation 1.3 vanishes, such that

$$\frac{11 - 2/3N_f}{4\pi}\,\alpha_s(Q^2)\,\log(\frac{\Lambda^2_{QCD}}{Q^2}) = -1. \tag{1.4}$$

Using this definition, equation 1.3 becomes

$$\alpha_s = \frac{4\pi}{(11 - 2/3N_f)\log(\frac{-q^2}{\Lambda_{\mathrm{QCD}^2}})}. \tag{1.5}$$

The value of Λ_{QCD} is around 200-300 MeV. This does not mean that the coupling constant is infinite at Λ_{QCD} , merely that the perturbative calculations used in the derivation of eqn 1.3 are no longer valid in this regime. When measured at the mass of the Z boson, the coupling constant $\alpha_s(M_Z) = 0.12$, indicating that perturbation theory is reliable at this energy scale.

A leading order diagram for a $qq \rightarrow qq$ process is shown in figure 1.2(a), where momentum is exchanged between two quarks via a gluon. At next to leading order (NLO), the gluon propagator in figure 1.2(a) may be replaced by the vacuum polarisation diagrams shown in figures 1.2(b)-1.2(d). The first of these diagrams, figure 1.2(b), causes the vacuum to effectively screen colour charge, such that at large distances the strength of the interaction is diminished. This is what happens in QED, and is the reason why

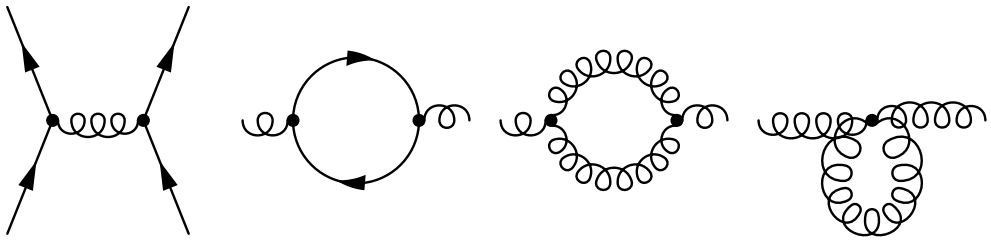

Figure 1.2: tree level qq qq scattering, and vacuum polarisation diagrams

the effective coupling constant α_{QED} decreases at higher momenta.

The three and four gluon vertices give rise to the diagrams in figures 1.2(c) and 1.2(d). The gluon loops in these diagrams cause an anti-screening effect, such that the strength of the interaction decreases as the exchanged momentum increases. This is the opposite effect to that seen for the quark loop, however in QCD it is this effect that dominates.

The anti-screening effect is characteristic of $SU(N)$ gauge theories. An $SU(4)$ theory would contain four colours and 15 gluon fields (N^2-1), increasing the contribution of the gluon loop diagrams in figure**??** and thus increasing the anti-screening effect. Conversely, there are only 3 gluon fields in an $SU(2)$ theory (c.f. the three gauge bosons of the weak force), which would result in a smaller anti-screening effect. The screening effect, however, increases with the number of quark fields contained in the theory. For example, in $SU(3)$ gauge theories that contain 17 or more quark flavours, the screening effect is dominant and the strength of the interaction increases as the exchanged momenta increases [5].

1.2.1 Factorisation

Computing the results of a proton-proton collision is complex, as different energy scales are involved in the problem. Them momentum exchanged between partons is at the TeV scale for collisions at the LHC, while the physics describing the arrangement of the partons within the proton is determined at a much lower scale, Λ_{QCD} . QCD is a strongly coupled theory at low energies, whereas at higher scales it is weakly coupled

and perturbative methods may be used. Fortunately, factorization allows the physics at these different scales to be separated [3]. The low momentum, nonperturbative physics describing the structure of the proton may be isolated from the high momentum, parton-parton scattering.

The structure of the proton may thus be described using Parton Distribution Functions (PDFs), $q_i(x,Q^2)$, $G(x,Q^2)$, and $\overline{q_i}(x,Q^2)$. The functions $q_i(x,Q^2)$ describe the probability of a probe with momentum Q^2 resolving a quark of flavour i within the proton, with said quark carrying a fraction x of the proton's momentum. Similarly, the distribution functions $\overline{q_i}(x,Q^2)$ and $G(x,Q^2)$ describe the probability of resolving an antiquark or gluon, respectively, within the proton. While a proton is typically thought of as containing two up quarks and one down quark, it also contains a number of gluons. These gluons may decay into quark-antiquark pairs, referred to as "sea" quarks. Because of this, the probabilities of finding antiquarks, or quarks with flavours other than up or down, are non-zero. The number of valence quarks is conserved, however, giving the conditions [2]

$$\int_0^1 dx \left[q_{\text{up}}(x,Q^2) - \overline{q_{\text{up}}}(x,Q^2)\right] = 2 \tag{1.6}$$

$$\int_0^1 dx \left[q_{\text{down}}(x,Q^2) - \overline{q_{\text{down}}}(x,Q^2)\right] = 1 \tag{1.7}$$

$$\int_0^1 dx \left[q_j(x,Q^2) - \overline{q_j}(x,Q^2)\right] = 0 \quad , \quad j \in \{c,s,t,b\} \tag{1.8}$$

While the parton distribution functions must be determined from experiment, the evolution of distribution functions can be calculated in a similar fashion to the coupling constant, α_s. The dependence of the PDFs on Q^2 is given by the Dokshitzer - Gribov - Lipatov - Altarelli - Parisi (DGLAP) equations[1, 2]:

$$\frac{\mathrm{d}q_i(x,Q^2)}{\mathrm{d}\log Q^2} = \frac{\alpha_s}{2\pi}\int_x^1 \frac{\mathrm{d}y}{y}\left[P_{qq}(y)q_i(\frac{x}{y},Q^2) + P_{qG}(y)G(\frac{x}{y},Q^2)\right] \quad (1.9)$$

$$\frac{\mathrm{d}\overline{q_i}(x,Q^2)}{\mathrm{d}\log Q^2} = \frac{\alpha_s}{2\pi}\int_x^1 \frac{\mathrm{d}y}{y}\left[P_{qq}(y)\overline{q_i}(\frac{x}{y},Q^2) + P_{qG}(y)G(\frac{x}{y},Q^2)\right] \quad (1.10)$$

$$\frac{\mathrm{d}G(x,Q^2)}{\mathrm{d}\log Q^2} = \frac{\alpha_s}{2\pi}\int_x^1 \frac{\mathrm{d}y}{y}\left[P_{Gq}(y)\sum_i\left(q_i(\frac{z}{y},Q^2) + \overline{q_i}(\frac{x}{y},Q^2)\right) + P_{GG}(y)G(\frac{x}{y},Q^2)\right], \quad (1.11)$$

where the P_{xx} are splitting functions. While a probe at Q^2 may resolve a quark or gluon within the proton, a probe with higher momentum may be able to resolve finer structures that are only present for a short time. For example, a given probe may be able to resolve a quark, while a probe with higher momentum may be able to interact with a collinear gluon emitted by this quark (fig 1.3(a)). Similarly, a high momentum probe may be able to resolve a quark or antiquark produced by a gluon (fig 1.3(b)). The splitting function $P_{Gq}(y)$ describes the probability that a gluon will be resolved a quark, carrying a fraction y of the quark momentum. Similarly the function $P_{qq}(y)$ describes the probability of resolving a daughter quark from a parent quark, while the functions $P_{qG}(y)$ and $P_{GG}(y)$ describe the probability of resolving quarks and gluons, respectively, from a parent gluon.

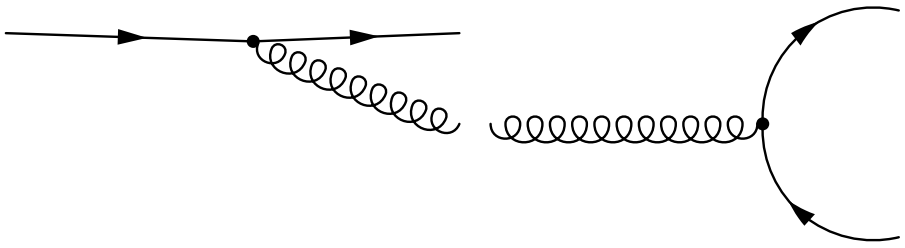

(a) (b)

Figure 1.3: processes described by the splitting functions. In figure 1.3(a), a quark emits a collinear gluon. A high momentum probe may be able to resolve the emitted gluon.

The PDFs derived by the CT10 group are plotted in figure 1.4. At small x the gluon

PDF is dominant, and consequently the sea quark contributions are also significant in this regime, whereas the valence quarks dominate at higher values of x.

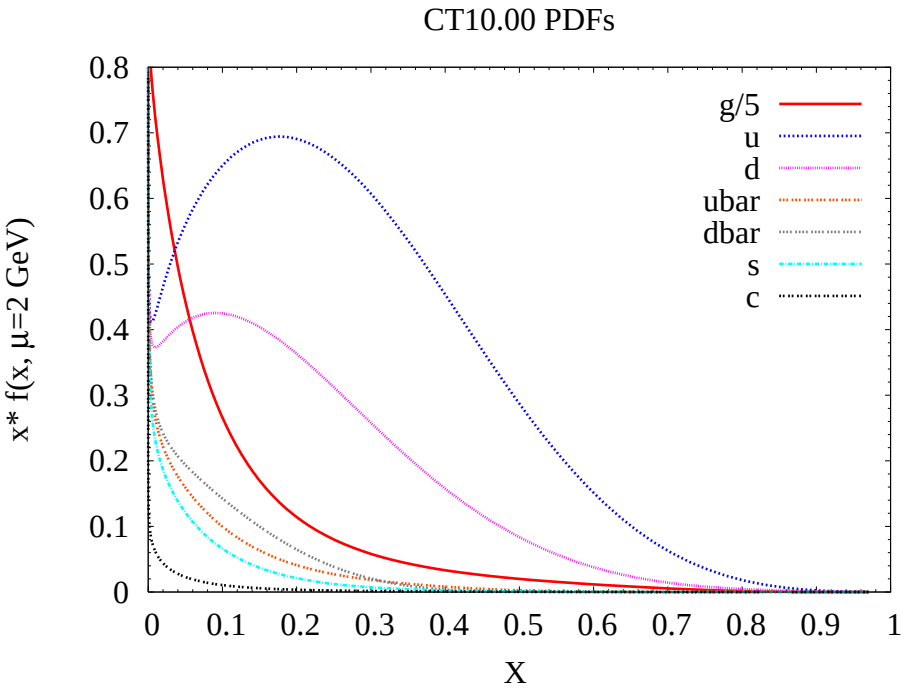

Figure 1.4: CT10 pdfs, obtained at a momentum scale of 2 GeV [6, 7].

1.2.2 Hadronization and Jet Production

Any partons produced in a collision will continue to interact via the colour force. However, the strength of the coupling increases approximately linearly with the separation between these partons: $\alpha_s \sim \sigma r$. This increases the probability that an initial parton will collinearly radiate other partons, in a process referred to as showering. While there may initially be only a few partons produced by the hard scattering, those partons will multiply, evolving into several collimated showers of partons.

These partons will then arrange themselves into hadrons. The confinement hypothesis states that colour charged partons do not exist in isolation, they must be confined within colourless hadrons. All hadrons observed in nature consist of quarks and gluons arranged

in colour singlet (i.e. neutral) states. If a given quark were to be separated from the other constituents in its parent hadron in order to "isolate" it, the energy required to achieve this would increase with the separation distance. At a certain point it becomes energetically favourable for a quark-antiquark pair to be produced from the vacuum, such that the remnants of the parent hadron form a bound state with one member of the new pair, while the separated quark binds with the other member of the pair. It is thus not possible to observe a free quark in isolation, as new hadrons are formed instead using partons created from the vacuum.

Partons created in the collision thus organise themselves into collimated sprays of hadrons, which are referred to as "jets". The showering and hadronization of particles are non-perturbative processes, and so it is difficult to predict the way in which a parton produced in a collision will evolve into a jet. In ATLAS, jets are defined from energy deposited in the calorimeters using jet finding algorithms, which are discussed in section **??**. The experimental measurement of the inclusive jet cross section obtained using 2010 data is discussed in section **??**.

Bibliography

[1] G. Altarelli and G. Parisi. "Asymptotic freedom in parton language". In: *Nuclear Physics B* 126.2 (1977), pp. 298 –318. ISSN: 0550-3213. DOI: 10.1016/0550-3213(77)90384-4. URL: http://www.sciencedirect.com/science/article/pii/0550321377903844.

[2] C.P. Burgess and G.D. Moore. *The Standard Model: A Primer*. Cambridge University Press, 2007. ISBN: 9780521860369.

[3] John C. Collins, Davison E. Soper, and George Sterman. "Factorization for short distance hadron-hadron scattering". In: *Nuclear Physics B* 261.0 (1985), pp. 104 –142. ISSN: 0550-3213. DOI: 10.1016/0550-3213(85)90565-6. URL: http://www.sciencedirect.com/science/article/pii/0550321385905656.

[4] *Combination of Higgs Boson Searches with up to 4.9 fb-1 of pp Collisions Data Taken at a center-of-mass energy of 7 TeV with the ATLAS Experiment at the LHC*. Tech. rep. ATLAS-CONF-2011-163. Geneva: CERN, 2011.

[5] W. Greiner, S. Schramm, and E. Stein. *Quantum Chromodynamics*. Springer, 2007. ISBN: 9783540485346. URL: http://books.google.ca/books?id=iNev7iHHG_MC.

[6] Hung-Liang Lai et al. *CT10 global analysis, additional figures and results*. 2012. URL: http://hep.pa.msu.edu/cteq/public/ct10/figs/.

[7] Hung-Liang Lai et al. "New parton distributions for collider physics". In: *Phys.Rev.* D82 (2010), p. 074024. DOI: 10.1103/PhysRevD.82.074024. eprint: 1007.2241.